

Article

Fatigue Assessment of Explosive Bolts Considering Vibration of Fixtures

Lixu Wang^{1,2}, Yang Zhao^{1,*}, Tieqiang Gang^{3,*}, Lijie Chen³ and Hongyu Tian³

¹ Department of Aerospace Engineering, Harbin Institute of Technology, Harbin 150001, China; lixuwang11@126.com

² Beijing Institute of Aerospace System Engineering, China Academy of Launch Vehicle Technology, Beijing 100076, China

³ Department of Propulsion Engineering, Xiamen University, Xiamen 361005, China; chenlijie@xmu.edu.cn (L.C.); tianhongyucyy@gmail.com (H.T.)

* Correspondence: yangzhao@hit.edu.cn (Y.Z.); gangtq@xmu.edu.cn (T.G.);
Tel.: +86-451-8640-2079 (Y.Z.); +86-592-218-4310 (T.G.);
Fax: +86-451-8640-2079 (Y.Z.); +86-592-218-9426 (T.G.)

Academic Editors: César M. A. Vasques and Giuseppe Lacidogna

Received: 9 November 2016; Accepted: 20 March 2017; Published: 3 April 2017

Abstract: In order to comprehensively evaluate the safety and reliability of a missile, this paper gives a process of how to perform fatigue assessment for release devices—such as explosive bolts—considering road roughness during its carrying on different classes of roads. Firstly, displacement power spectral density (PSD) function is used to fit models of road surfaces of Class A, C, and E. Taking the surface models as simulations, multi-body dynamics analyses with code ADAMS are performed to obtain acceleration responses of different points on the missile. Loading these accelerations, the corresponding stress distribution of explosive bolts is achieved with FEM code ABAQUS. These loads are counted by rainflow method. Finally, constant life curves with different survival rates are employed to get the S-N curves at different stress ratios and stress concentration coefficients, and fatigue lives of explosive bolts are assessed based on the stress-life method. Afterward, the effect of pretension force on the vibration load is obtained. This paper provides a fatigue evaluation procedure for release devices, which is helpful to raise the reliability of release devices for both design and service procedures.

Keywords: explosive bolt; fatigue assessment; fatigue life; stress-life method

1. Introduction

Explosive bolts are typical pyrotechnic release devices used for diverse applications, including launcher operation, rocket sled release, etc. [1–4]. Compared with normal bolts, an explosive bolt usually has a cavity filled with a removable cartridge or an explosive charge. By detonating the explosives, a shock wave is generated and the explosive bolt is broken so as to realize multistage separation between interfaces. Hence, the separation reliability is of great significance for release devices.

The reliability, efficiency, and design of explosive bolts has been studied [1,4–6]. Juho Lee et al. [1,4] established separation behavior analysis environments for ridge-cut explosive bolts and verified the numerical analysis method, including appropriate failure criteria. Their works focused on the separation mechanism and design parameters of explosive bolts. Syed Haider Abbas et al. [5] proposed a non-contact, multipoint, and remote pyroshock measurement system to measure the pyroshock waves generated, which is very important to understand the characteristics of pyroshock on the host structure. Peng Gao et al. [6,7] proposed dynamic reliability models based on equivalent strength

degradation paths and discussed the dynamic reliability analysis of explosive bolts in the launch process of satellites. Most of the literature has focused on the reliability of the structures in the exploding procedure and static strength design problems.

Yet, for missile devices, this reliability issue should cover the procedure of long-distance carrying on vehicles. In this procedure, missile vehicles experience alternating road surfaces. In addition to the vehicle parts, the missile and its connecting explosive bolts also undergo vibrations, which may cause fatigue damage and result in the failure of the release device. This connecting reliability is affected by the pretension force, structural geometry, failure probability of materials, and so on. Thus, it needs a comprehensive safety analysis. So far, no literature outlines how to design and prevent fatigue failure or how to perform fatigue assessments for explosive bolts.

Thus, in this article we state the process to evaluate the fatigue of explosive bolts on missiles during carrying on roads of Class A, C, and E. First, road roughness curves are generated via the displacement power spectral density (PSD) function according to ISO standard. Dynamics analyses are then performed by code ADAMS to obtain acceleration responses of different points on the vehicle, and the corresponding stress distribution of explosive bolts are calculated with FEM code ABAQUS. Finally, the fatigue life of the explosive bolt is evaluated by the stress-life method.

2. Generation of Road Surface Spectrum

Road roughness function $x_m(L)$ is generally defined as the variation of height x_m of a road surface to a reference plane along road length L [8]. Stochastic data of road roughness are measured and processed to obtain a displacement PSD $G_x(n)$.

According to ISO 8608: 1995 [9],

$$G_x(n) = G_x(n_0) \left| \frac{n}{n_0} \right|^{-\omega} \tag{1}$$

$G_x(n)$ is namely road roughness factor. On the basis of displacement PSD, road surfaces are divided into eight classes from A to H. n is spatial frequency, i.e., the number of wavelengths per meter, n_0 a reference value of n , and ω an exponent of fitted PSD. $G_x(n_0)$ is the road roughness value at n_0 , which is a constant for a given road class. From the national standard [9], $n_0 = 0.1 \text{ m}^{-1}$ and $\omega = 2$.

If a road is sampled N times with an interval ΔL , the total sampling length is $L = N\Delta L$ and the spatial frequency resolution is $\Delta n = 1/L$. With the discrete Fourier transform, the obtained data $x_m (m = 0, 1, \dots, N - 1)$ is transformed to

$$X_k = \sum_{m=0}^{N-1} x_m e^{-\frac{j2\pi km}{N}} (k = 0, 1, \dots, N - 1). \tag{2}$$

The relationship between X_k and the displacement PSD $G_x(n_k)$ is [10]

$$|X_k| = \sqrt{\frac{N}{2\Delta L} G_x(n_k)} \left(k = 0, 1, \dots, \frac{N}{2} \right), \tag{3}$$

where $n_k = k\Delta n$. Equation (3) gives the modulus value of the discrete Fourier transform. Suppose the phase angle is φ_k , randomly selected in $[0, 2\pi]$, then

$$X_k = |X_k| e^{j\varphi_k} \left(k = 0, 1, \dots, \frac{N}{2} \right). \tag{4}$$

In Equation (4), only the first $\frac{N}{2} + 1$ terms are transformed by the discrete Fourier transform, in which $X_0 = \sum_{m=0}^{N-1} x_m$. Through mean normalization, we have $X_0 = 0$, and then X_1 and X_{N-1} , X_2 and $X_{N-2}, \dots, X_{\frac{N}{2}-1}$ and $X_{\frac{N}{2}+1}$ are respectively conjugate.

Performing the discrete inverse Fourier transform for X_k , we get [11]

$$x_m = \frac{1}{N} \sum_{k=0}^{N-1} X_k e^{\frac{j2\pi km}{N}} \quad (m = 0, 1, \dots, N - 1). \tag{5}$$

Statistical data shows that most of the highways in China belong to Class A, B, and C [12]. So, in this paper Class A is taken as an ideal condition, Class C as a common one, and Class E as a severe one. We then simulate the road roughness and correspondingly study the dynamical response of the missile vehicle in maneuver.

Due to the existence of the vehicle vibration isolation system, the spatial frequency n is sampled within the range of (0.011, 2.830) [13]. Here, the sampling length is $L = 600$ m with an interval $\Delta L = 0.1$ m. From Ref. [9], $G_x(n_0)$ is $16 \times 10^{-6} \text{ m}^3$, $256 \times 10^{-6} \text{ m}^3$, and $4096 \times 10^{-6} \text{ m}^3$ for Class A, C, and E roads, respectively. For each class, the same random sequence is used for phase angle φ_k in Equation (3). Hence the road roughness of different classes changes proportionally and the ratio is $x_A : x_C : x_E = 1 : 4 : 16$, as plotted in Figure 1.

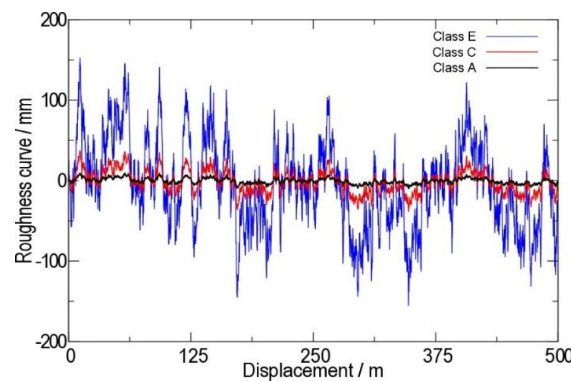


Figure 1. Road roughness curves of Class A, C, and E.

3. Dynamics Analysis of the Missile Vehicle Based on ADAMS

The missile vehicle is simplified as shown in Figure 2. The DOFs of Y translational degree of freedom—the rotation degree of freedoms about axis X and Z , ROT X and ROT Z —are set to zero. The chassis is simplified as a rigid body, the suspension systems are described as Spring-Damping systems, and the Pacejka 89 tire model is picked to simulate the tire.

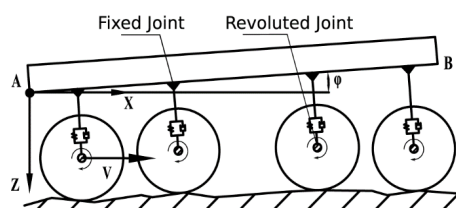


Figure 2. Simplified vehicle model for the dynamics analysis.

The suspension systems are constrained to the chassis with fixed joints, and all DOFs of these joints are constrained to zero. The tire and the suspension system are constrained with revolute joints at the center of the tire, where only the DOF of ROT Y exists.

Suppose that the rear wheels be driven at a constant speed of 12 m/s along axis X and that the riven torque has not been taken into consideration, by supposing the vehicle drives at a constant speed. Because the vehicle drives at a relatively low speed, we suppose the tires and the road surface be kept in contact during the whole transportation process.

The road surfaces obtained in Section 2 are used as the excitation in the vehicle dynamic simulation to produce longitudinal displacement X , vertical displacement Z , and pitch angle ϕ . The suspension is modeled by a damping-spring system. Magic tire Pacejka89 in ADAMS is picked as the tire model. The related parameters of the missile and its vehicle are listed in Table 1.

Table 1. Parameters of the missile and the carrying vehicle.

Components	Conditions	Parameters
Assembly	Drive mode	8×2
	Wheelbase	$(1600 + 3500 + 1600)$ mm
	Body mass	18,300 kg
	Center-of-mass coordinate	$(3294.2, 305.1, 0)$ mm
	The moment of inertia to centroid	$56,178,826,615$ kg·mm ²
Suspension	Suspension type	Rigid axle suspension
	Mass	200 kg
	Stiffness coefficient	300 N/mm
	Damping coefficient	5 N·s/mm
Tire	Mass	25 kg
	Free radius	671.5 mm
	Aspect ratio	0.35
	Longitudinal stiffness coefficient	300 N/mm
	Longitudinal damping coefficient	1.6 N·s/mm
Warhead and missile body	Connection mode	Explosive bolts connection
	Number of connections	4
	Position of connections	Quadrantal points of a $\phi 840$ mm circle

The virtual prototype of the missile and the carrying vehicle are assembly-built by the dynamics analysis software ADAMS, as shown in Figure 3. Here, we suppose the total mass (including missile body, warhead, filler, and structures inside) of the missile is about 8300 kg; 1000 kg for the warhead and filler inside, and 7300 kg for the missile body and structures inside. The filler inside mainly affects the performances of the vehicle more, such as rollover. Our research focuses on the safety of the explosive bolt, so we neglect the effect of the filler and other structures inside, and construct a model according to mass equality. This simplification makes it more convenient to analyze the structures we are interested in, namely the explosive bolts.

Since we are interested only in the effect of road roughness on the carrying structure’s loading, instead of the dynamic process and performance of the vehicle, for the convenience of analysis we suppose the missile vehicle drives at a speed of 12 m/s on Class A, C, and E roads, and the wheelbase and the road surface are constrained coplanar in X - Z plane so as to remain in a linear motion. Performing dynamical analysis, we obtain the longitudinal, vertical, and pitch angle accelerations of point A on the missile vehicle when driven on Class A, C, and E roads, as shown in Figure 4.

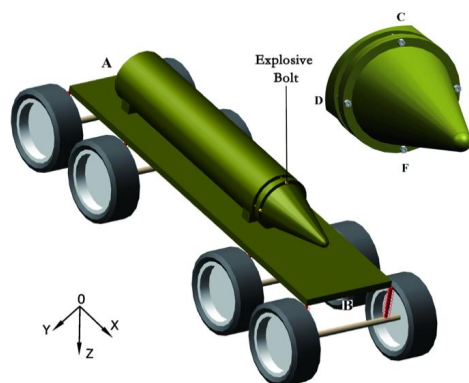


Figure 3. ADAMS prototype of missile vehicle.

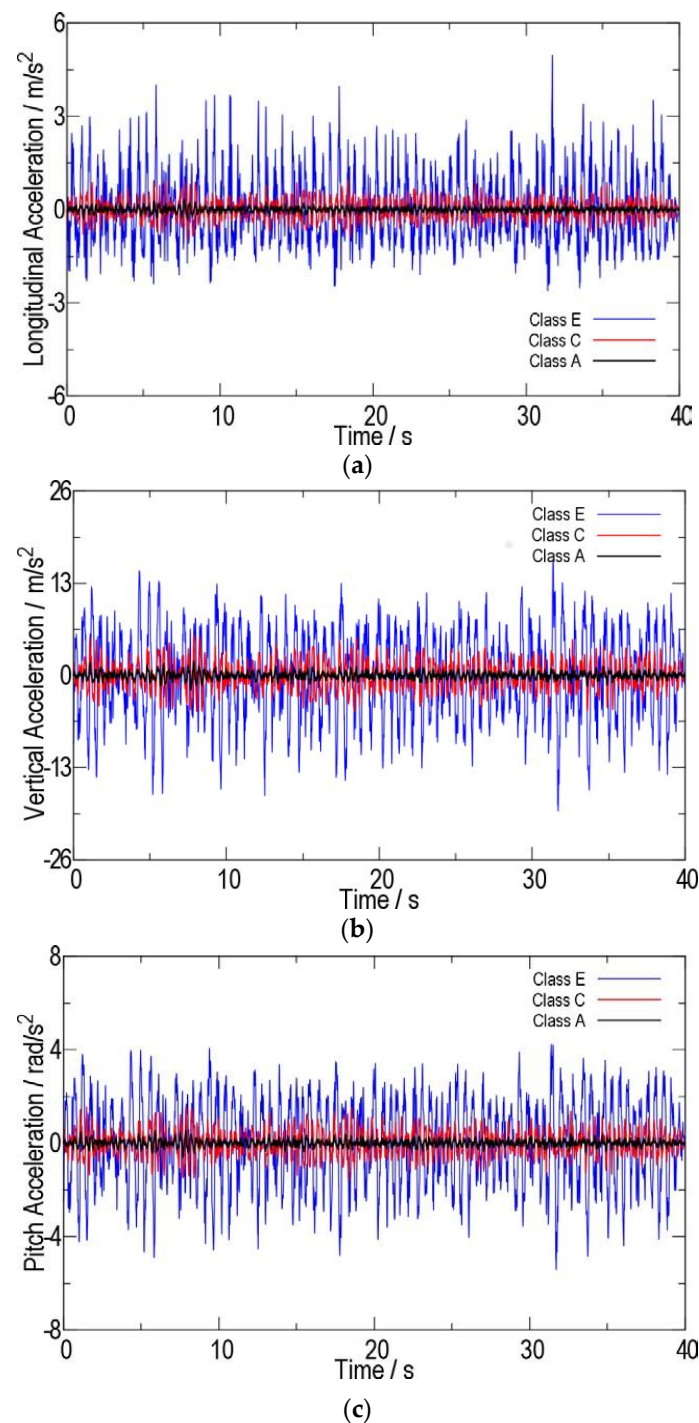


Figure 4. (a) Longitudinal, (b) vertical, and (c) pitch angle accelerations of point A on the missile vehicle when driving on Class A, C, and E roads.

4. Mechanical Behavior Analysis of Explosive Bolts Based on FEM

In order to obtain the stress responses of explosive bolts during vibrations on roads, we model the assembly of vehicle frame, warhead, missile body, explosive bolts, and nuts together. The FEM model is shown in Figure 5. The local meshes around the weaken groove are refined to get the mesh convergence. Properties and convergent meshes of the whole geometry missile model are listed in Table 2. Contacts and constraints of the missile vehicle are assigned as listed in Table 3.

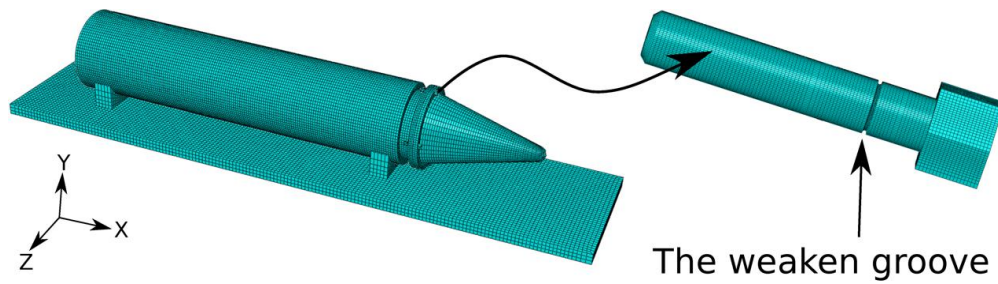


Figure 5. Meshes of the half missile model.

Table 2. Properties and meshes of the half missile model.

Parts	Material Properties				Element Type	Number of Elements
	Density (kg/m ³)	Elastic Modulus (GPa)	Poisson's Ratio	Ultimate Tensile Strength σ_b (MPa)		
Vehicle frame	7800	210	0.3	410	C3D8R	22,755
Warhead	7800	210	0.3	410	C3D8R	8092
Missile body	7800	210	0.3	410	C3D8R	80,013
Explosive Bolt	7790	211	0.3	1570	C3D8R, C3D6	91,128
Nut	7790	211	0.3	1570	C3D8R	5832

Table 3. Contacts and constraints sets of missile vehicle.

Parts	Constraints	Friction Coefficient
Warhead-missile body	Surface-surface contact	0.15
Explosive bolt-warhead	Surface-surface contact	0.15
Nut-missile body	Surface-surface contact	0.15
Explosive bolt-nut	Binding constraints	-
Missile body-vehicle frame	Binding constraints	-

The pretension force of explosive bolts are assigned as $F_{pre} = 0.4 \sigma_b A_s$, where A_s is the area of the dangerous cross-section, i.e., the root section of the weakened groove. Thus, the pretension force is $F_{pre} = 180$ kN. In this paper, for the complexity of the system we simplify the model and the loads. Suppose that the wheels will experience the same road surface model if they are at the same longitudinal position at the same time. Neglecting the loads of lateral (along Z axis), yaw angle (about Y axis) and roll angle (about X axis), the loads are applied by the longitudinal, vertical, and pitch angle accelerations (about Z axis), a_x , a_y , and a_α , of the missile vehicle obtained in Section 3, as noted in Figure 6.

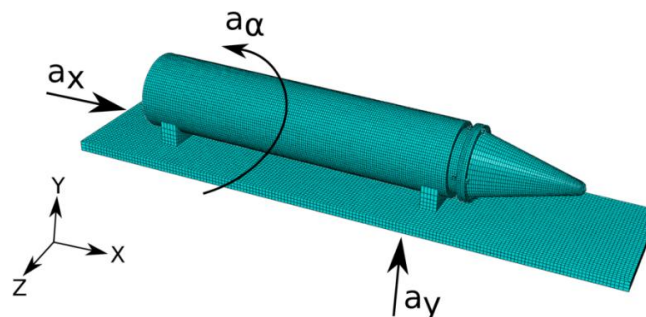


Figure 6. Loads of the missile vehicle.

Because the Class E road is the most serious condition, we take this to present our results. Figure 7 gives the typical Tresca stress distribution at the weakened groove of bolt C when driving at the Class E road. In our calculation results, the Tresca stress is obviously larger than the Mises stress. Thus,

it will be safer to take the Tresca stress as referring to the maximum shear stress strength theory into account to assess the fatigue of the explosive bolts. The maximum Tresca stress is 1222.32 MPa at the root of the groove, namely the dangerous point, which is lower than the conditional yield strength $\sigma_{0.2} = 1480$ MPa. Thus, the explosive bolt is fully in an elastic deformation state. Figure 8 presents the variation of the Mises and Tresca stress of the dangerous point on the explosive bolt C with time. It shows that the stress varies in small amplitude and that the maximum amplitude is about 14 MPa under the design pretension force. This is because of the existence of enough pretension force and the friction produced between contact surfaces.

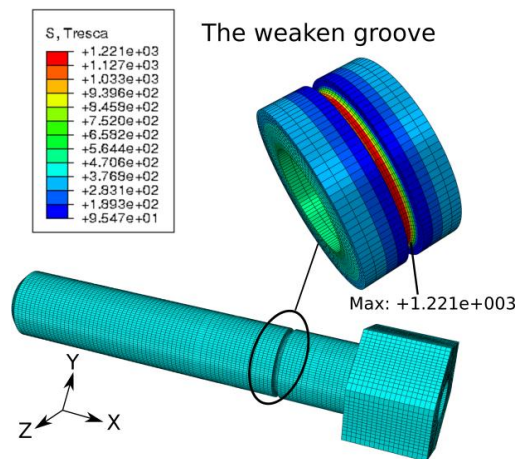


Figure 7. Typical Tresca stress distribution at the weakened groove of the explosive bolt C under Class E road.

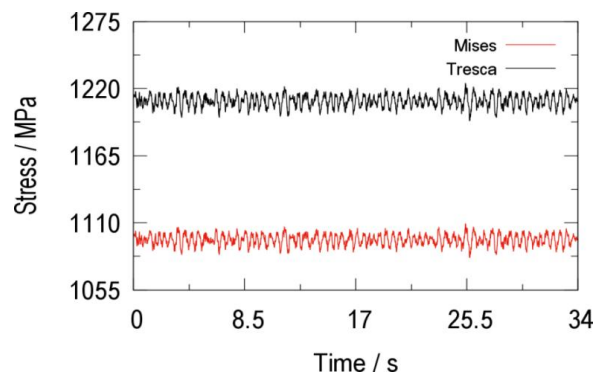


Figure 8. Variation of the Mises and Tresca stress of the dangerous point on explosive bolt C with time under Class E road.

5. Fatigue Life Assessment of Explosive Bolt

The Mises and Tresca stress response of the dangerous point on explosive bolt C when driving on different class roads are counted by rainflow method [14]. The extreme condition, Class E road, is taken as an example to explain the fatigue assessment process during the carrying of the missile.

It is required that the key release devices will not fail during the 6000 km carrying distance. We take a stress-time response of FEM analysis shown in Figure 8 as a load block, i.e., 400 m carrying distance, ignoring the unstable period induced by the startup. According to Miner’s rule, the fatigue life of the explosive bolt is required to be larger than the 15,000 load block.

The obtained 178 cyclic stresses rank in an ascending order by stress ratio R , ranging from 0.9777 to 0.9975. Table 4 lists only the first five cyclic Tresca stresses for references.

Generally, fatigue damage produced by vibration during driving of a vehicle is a high cycle fatigue issue. Thus, the stress-life method based on S-N curve can express the vibration fatigue life varying with loads by a three-parameter model as

$$N = A(\sigma_{\max} - \sigma_0)^b \tag{6}$$

where N is the number of stress cycles, i.e., life, and σ_{\max} the applied maximum stress. A , b , and σ_0 are constants.

Referring to the axial-fatigue testing data of 30GrMnSiNi2A in [15], the constant life curves of $K_t = 3$ and $K_t = 5$, and the S-N curve at $K_t = 1$ and $R = 0.1$ based on median fatigue life, are given, as plotted in Figures 9–11. In Figure 11, we also give the S-N curves at $K_t = 1$ and $R = 0.1$ with different survival rates P . Concerning Figures 9–11, through linear interpolation, we can get the constant life curves at any given K_t , P , and R . Figure 12 shows the constant life curve of $N = 10^7$ at different K_t and P , and the dashed curves are obtained through linear interpolation.

Among all of the 178 cyclic stresses, $R_{\min} = 0.9777$. The corresponding fatigue limit is 1490 MPa, based on fatigue life curve for 99.99% survival rate, which is the minimum one with R ranging from 0.9777 to 0.9975. However, as we counted, the maximum stress of all the cycles is 1222.32 MPa, lower than the minimum fatigue limit. Hence, based on fatigue life curve for 99.99% survival rate, fatigue damage will not occur when driving on Class E roads and no fatigue damage accumulated. Consequently, with the designed geometry and pretension force in this paper, these explosive bolts can undergo more than 15,000 load blocks, i.e., 6000 km carrying distance on Class A to E roads.

Table 4. Rainflow counting results of Tresca stress.

No.	Stress Amplitude/MPa	Max Stress/MPa	Cycle	Stress Ratio
1	13.650	1222.320	0.5	0.9777
2	13.475	1222.320	0.5	0.9780
3	13.110	1221.590	0.5	0.9785
4	12.570	1220.160	0.5	0.9794
5	12.505	1221.420	1.0	0.9795

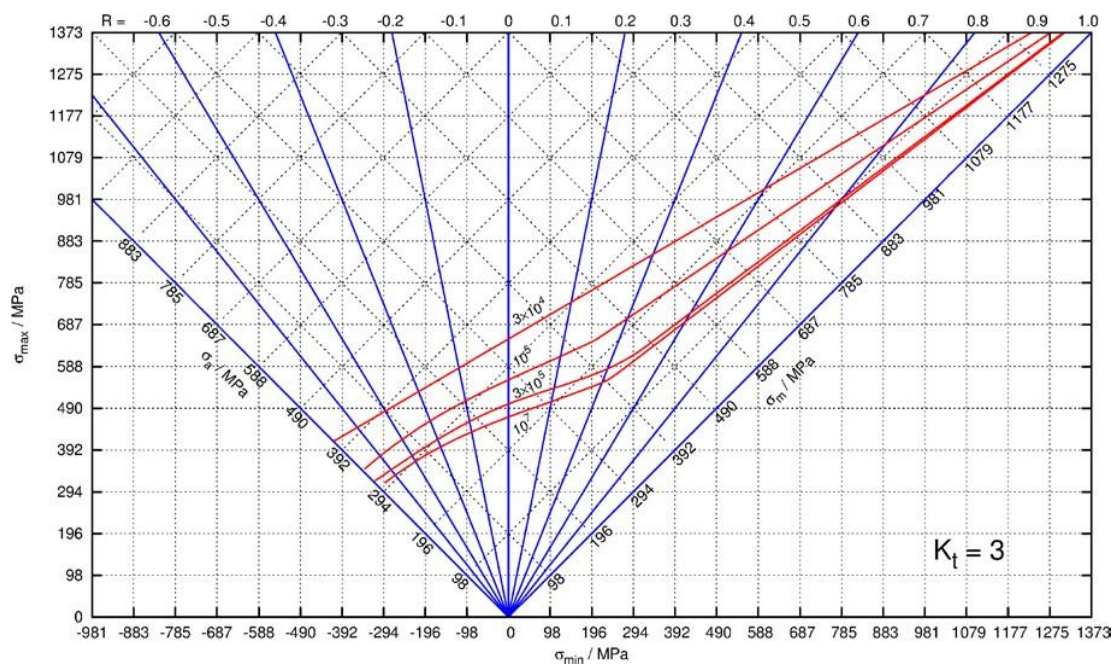


Figure 9. Constant life curve of $K_t = 3$ based on median fatigue life.

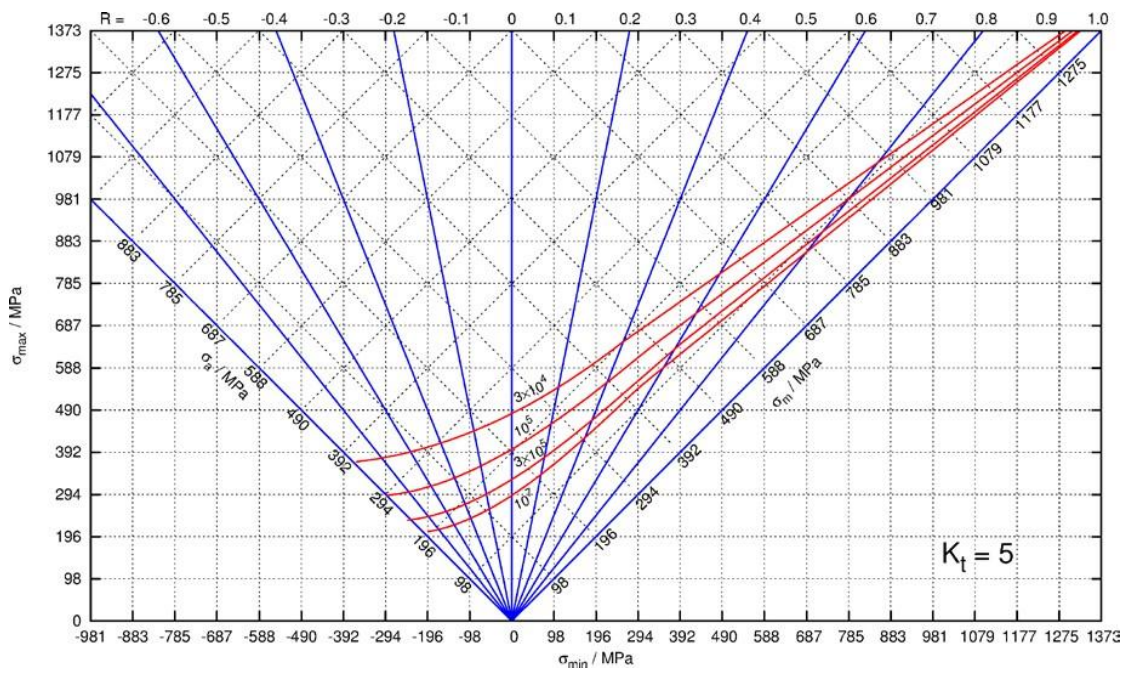


Figure 10. Constant life curve of $K_t = 5$ based on median fatigue life.

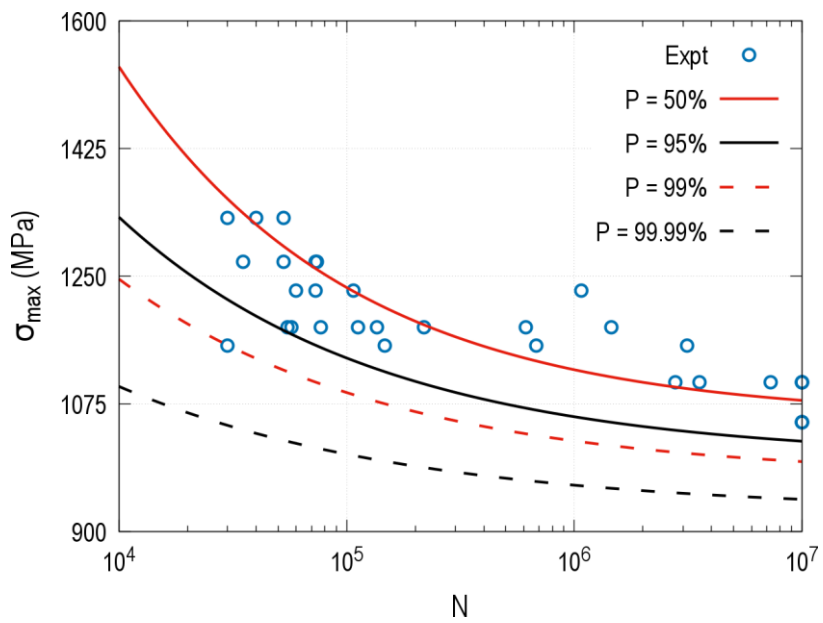


Figure 11. S-N curves of $K_t = 1$, $R = 0.1$ with different survival rates.

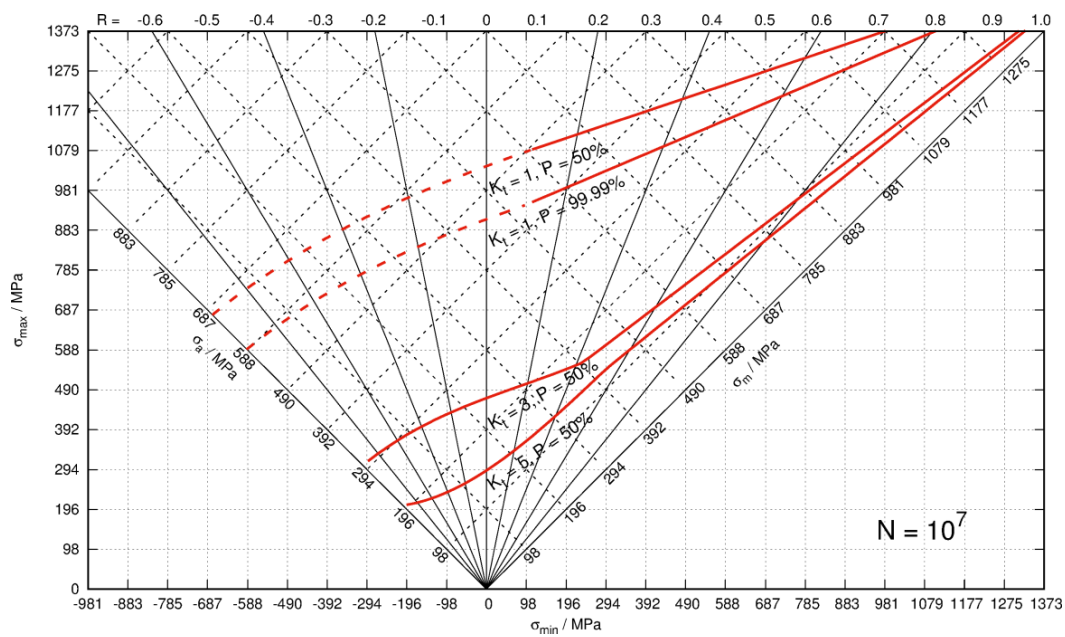


Figure 12. Constant life curve of $N = 10^7$ with different survival rate.

6. Discussion

Since the missile vehicle and the release device are complex systems, the fatigue strength of the explosive bolts will be affected by the pretension force, the depth of the weakened groove, the road roughness, the fatigue life curve with a certain failure probability, and so on. Based on the above results, we can find when the pretension force of explosive bolts are assigned as $F_{pre} = 0.4\sigma_b A_s$, the vibration amplitude is relatively small; i.e., maximum amplitude is about 14 MPa and the corresponding stress ratio is 0.9777.

In order to ensure the explosive bolts will not break during the missile transportation on the vehicle, we analyze the effects of pretension force on the vibration behavior of the structure, as illustrated in Figure 13. It reveals that the minimum stress ratio obviously decreases with the decreasing of the pretension force (from $0.4\sigma_b A_s$ to $0.2\sigma_b A_s$) in the whole vibration response, while the maximum vibration amplitude increases linearly. Still following the analysis process in Section 5, we obtain that these explosive bolts can undergo more than 6000 km carrying distance on Class A to E roads.

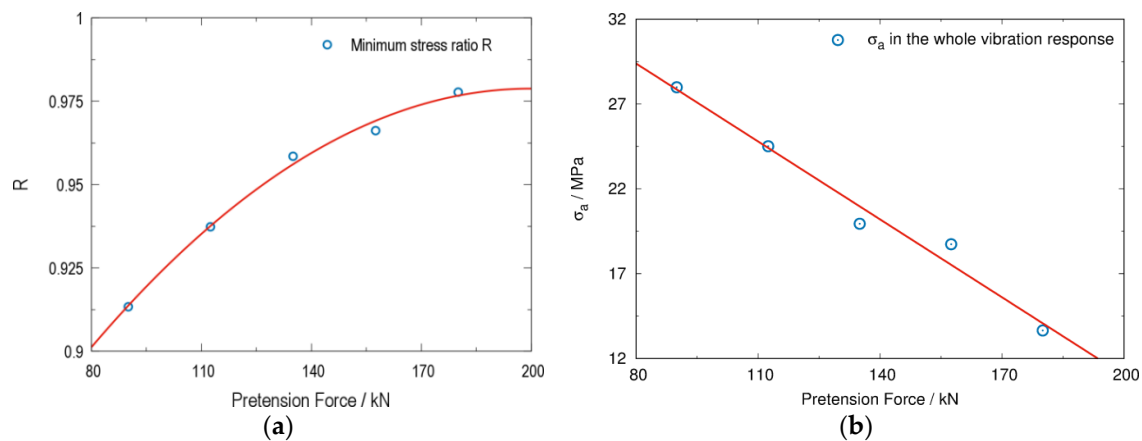


Figure 13. The variation of (a) the minimum stress ratio R ; and (b) the maximum stress and stress amplitude with the decreasing of the pretension force in the whole vibration response of the bolts.

Except for the pretension force, there are still other factors that will influence structural safety, such as the design of the wall thicknesses of the weaken groove and the charge hole, and the dispersion of mechanical behavior of the material. From this work, we provide a possible process to assess the fatigue safety of this complex system. When there is a possibility of facing fatigue fracture, it is recommended that the diagram of Figure 14 be followed to conduct fatigue evaluations or redesign the structure to improve safety. Also, further detailed material tests and structural optimization analyses are needed to ensure high-reliability safety.

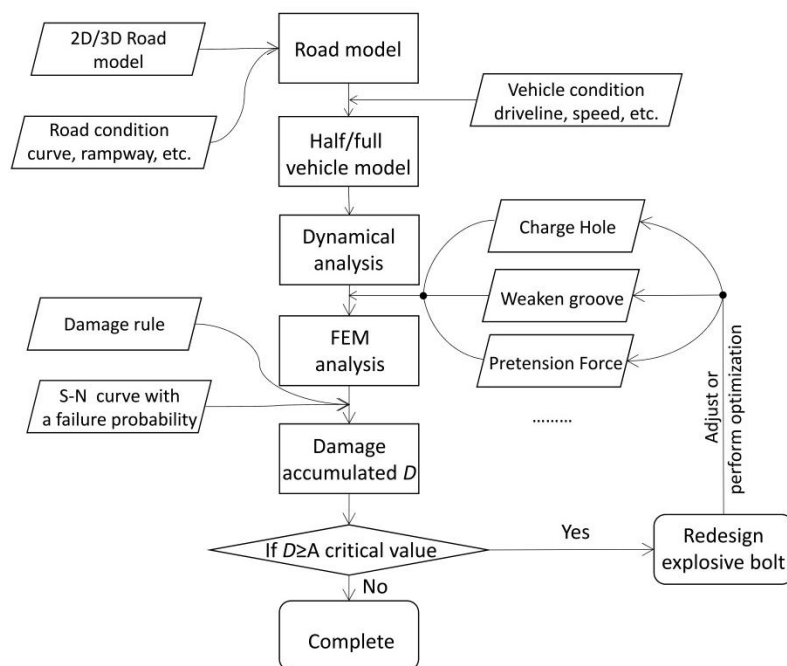


Figure 14. The diagram of fatigue assessment and redesign procedure.

7. Conclusions

- (1) Road roughness curves of Class A, C, and E are generated based on the displacement PSD. The road roughness of different classes based on the same random sequence change proportionally, and the ratio is $x_A : x_C : x_E = 1 : 4 : 16$. The corresponding longitudinal, vertical, and pitch angle accelerations of the missile vehicle are obtained when driving on roads of Class A, C, and E, as shown in Figure 4a–c for point A.
- (2) Counted with rainflow counting method, the stress ratio R at the root of the explosive bolt ranges from 0.9777 to 0.9975, and the maximum stress of all the cycles is 1222.32 MPa, which is lower than the corresponding minimum fatigue limit for a survival rate of 99.99%. Thus, with the designed geometry and pretension force in this paper, these explosive bolts can undergo more than 15,000 load blocks, i.e., 6000 km carrying distance on Class A to E roads.
- (3) With the pretension force decreasing from $0.4\sigma_b A_s$ to $0.2\sigma_b A_s$, the minimum stress ratio obviously decreases, while the maximum vibration stress amplitude increases linearly. When facing a fatigue fracture issue, it is recommended to follow the diagram of Figure 14 to redesign the structure.

Acknowledgments: The authors would like to thank the support of the National Natural Science Foundation of China (No. 51475396), the National Basic Research Program of China (No. 2013CB733004), and Natural Scientific Research Innovation Foundation in Harbin Institute of Technology (No. 30620150071).

Author Contributions: Lixu Wang, Lijie Chen and Hongyu Tian did the simulations and wrote the paper; Yang Zhao, Tieqiang Gang, and Lijie Chen gave the basic idea about the analysis process and did the discussions of the main results; all the authors revised the paper together.

Conflicts of Interest: The authors declare no conflict of interest.

References

1. Lee, J.; Han, J.; Lee, Y.; Lee, H. Separation characteristics study of ridge-cut explosive bolts. *Aerosp. Sci. Technol.* **2014**, *39*, 153–168. [[CrossRef](#)]
2. Bement, L.J.; Schimmel, M.L. *A Manual for Pyrotechnic Design, Development and Qualification*; NASA Technical Memorandum: Hampton, VA, USA, 1995.
3. Brauer, K.O. *Handbook of Pyrotechnics*; Chemical Publishing Co.: New York, NY, USA, 1974.
4. Lee, J.; Han, J. A parametric study of ridge-cut explosive bolts using Hydrocodes. *Int. J. Aeronaut. Space Sci.* **2015**, *16*, 50–63. [[CrossRef](#)]
5. Abbas, S.H.; Jang, J.; Lee, J.; Kim, Z. Development of an FPGA-based multipoint laser pyroshock measurement system for explosive bolts. *Rev. Sci. Instrum.* **2016**, *87*, 073302. [[CrossRef](#)] [[PubMed](#)]
6. Gao, P.; Yan, S.; Xie, L.; Wu, J. Dynamic reliability analysis of mechanical components based on equivalent strength degradation paths. *J. Mech. Eng.* **2013**, *59*, 387–399. [[CrossRef](#)]
7. Gao, P.; Yan, S. Fuzzy dynamic reliability model of dependent series mechanical systems. *Adv. Mech. Eng.* **2013**, *2013*. [[CrossRef](#)]
8. ASTM E867-02. *Terminology Relating to Vehicle-Pavement System*; ASTM International: West Conshohocken, PA, USA, 2002.
9. ISO 8608: 1995. *Mechanical Vibration—Road Surface Profiles—Reporting of Measured Data*; International Organization for Standardization: Geneva, Switzerland, 1995.
10. Liu, X.; Deng, Z.; Gao, F. Study of simulation of road roughness based on inverse transform. *China J. Highw. Transp.* **2005**, *18*, 122–126. (In Chinese)
11. Liu, X.; Deng, Z.; Gao, F. Research on the method of simulating road roughness numerically. *J. Beijing Univ. Aeronaut. Astron.* **2003**, *29*, 843–846. (In Chinese)
12. Wang, X.; Wang, B. Expressway pavement power spectral density. *J. Traffic Transp. Eng.* **2003**, *3*, 53–56. (In Chinese)
13. Yu, Z. *Automobile Theory*, 5th ed.; China Machine Press: Beijing, China, 2009. (In Chinese)
14. Nieslony, A. Determination of fragments of multiaxial service loading strongly influencing the fatigue of machine components. *Mech. Syst. Signal Process.* **2009**, *23*, 2712–2721. [[CrossRef](#)]
15. Editorial board of engineering materials manual. *Engineering Materials Manual: Structural Steel, Stainless Steel*; China Standards Press: Beijing, China, 1989; Volume 5. (In Chinese)



© 2017 by the authors. Licensee MDPI, Basel, Switzerland. This article is an open access article distributed under the terms and conditions of the Creative Commons Attribution (CC BY) license (<http://creativecommons.org/licenses/by/4.0/>).